

## Evaluation the Effect of Shot Peening Time on Static Torsional Strength of AA7178-T6

Ali Hassan Saleh Shatha, M. Rajaa Abduljabbar,  
Adnan Namaa Abood and Hassan A. Abdulhadi  
Insitute of Technology, College of Engineering and Technology,  
Middle Technical University, Baghdad, Iraq

**Abstract:** In the current study, the effect of shot-peening on the static torsional strength of AA7178-T6 was investigated. Time of shot-peening was adopted as a varied parameter to evaluate its effect on plastic state in static torsion test of alloy. Residual stresses and surface roughness was measured to indicate the influence of shot-peening time on alloy surface state. Torque predicted was calculated to evaluate the elastic torque and plastic torque values according to shot-peening parameter. The results show that the shear strain decreases whenever shot-peening time increase especially when up to 30 min that shear strain reduced by 45% and plastic torque predicted also decreased at this time by 10% compare to its values of specimen without peened which means that the strength of alloy improved with this process while shear stress decreased by 3.84% at this condition. The total torque predicted was closed to experimental torque with average variation 14%. Experimental torque decreased by 3.84% with the increasing of shot-peening time.

**Key words:** Torsion test, shot-peening, AA7178-T6, plastic torque, elastic torque, torque predicted

---

### INTRODUCTION

AA 7178-T6 is one of Al-Zn-Mg alloys and considered high strength alloy that used in applications of aircraft structure because of containing Cu which improves the mechanical strength through precipitation hardening (Meng and Frankel, 2004). For these features of alloy, it was selected in the current work to study the improvement of its strength in static torsion test. Recently, many researchers interested in study the torsional strength of materials. Schiltges *et al.* (1998) presented a new static torsional test using silicon and metallic LIGA. They concluded that their work gives good results when carry out on silicon. Barthelat *et al.* (2002) presented an empirical methodology for the equasi-static and dynamic torsion testing on aluminum 6061-T6 coating with  $\text{Al}_2\text{O}_3/\text{TiO}_2$  and Wc/Co. They concluded that the difference between the Nano and micro-structured materials appeared through initial damage in the coatings while no important difference observed in modulus and strength. Orduna and Lourencos (2005) studied plastic torsion of arbitrarily shaped and proposed a general solution for equations governing its behavior. They concluded that the source of error can be reduced in the three dimensional limit analysis of structures according to their proposal. Jonathan *et al.* (2008) employed appropriate geometry to find values of fracture toughness

values without measurement of crack length through double torsion testing. They concluded that nonlinear effects were encountered in the plates of small thickness ( $W/d < 80$ ). Bidulska *et al.* (2007) used torsion test to study the effect of low strain rate on formability of aluminum alloy 2014. They found that the ductility decreased as strain rate ( $\dot{\epsilon}$ ) increased and Temperature (T) decreased.  $\dot{\epsilon} = 10^{-3} \text{ sec}^{-1}$  and  $T = 300^\circ\text{C}$  is an optimal condition. Bressan (2007) carried out high speed plastic torsion and low speed tensile test on pure copper and aluminum to investigate the plastic behavior, beginning of plastic instabilities and work hardening of cylindrical specimens. The results show that the strain rate sensitivity (m) increased ten folds for aluminum. Albuquerque and Rodrigues (2008) adopted double-torsion test and determined the dimensions of specimens to recognize the influence of thin test specimen with the results of this test. They concluded that the dimensions of test specimen or notch length did not cause variation of critical crack length. Mossakovsky *et al.* (2011) discussed the stress state of solid cylinder torsion test subjected to high strain rates and they found that this approach helped in constructive the fracture surface accurately. Diani *et al.* (2011) designed and built a device for torsion test to employ it for testing the shape fixing and shape recovery of shape memory polymers at large deformation. They concluded that torsion test represents

states of strains more accurately than traditional methods used uniaxial tension or compression deformations. Patil and Gore (2013) used different specimens geometry of 1020 steel and aluminum to present curves of torque-twist and true stress-strain and used ABAQS to simulate torsion tests. They concluded that the solid specimens are less reliable for torsion tests than tubular specimens. Roesler *et al.* (2014) correlated the values of torsion test variables with the molecular weight, numerical simulation and fracture surface of PLDLA 70/30 AC1 interface screws. They concluded that the mechanical properties of cannulated polymeric screws can be determined by torsion test. Vainikka *et al.* (2015) described the development and construction of a device for torsion testing of 3D-printed hollow plastic tubes. They found that cylindrically printed tubes broke in a 45° parallel to the main shear stress and this supports the idea that the new method provides tubes that can endure bigger shear strength. Saborowski *et al.* (2017) compared the results of shear stress obtained from two methods, lap shear test and butt bonded hollow cylinders of thermally joined aluminum-polyamide hybrid compounds. They concluded that the results of hollow cylinder torsion test are more reliable than results from the lap shear test. Nayak *et al.* (2018) used carbon/epoxy composite drive shaft to increase torsional strength compared to that of an OEM steel shaft. They concluded that the torsional strength increased by 8.5% along with a weight reduction of 60% and the carbon/epoxy shaft can successfully be used to replace OEM steel shaft.

**Theoretical principles:** In the torsion test, the shear strain only increases linearly after yielding occur. The elastic region called an “elastic core” and the distribution of shear stress is nonlinear outside of this core because of starting of plastic zone (Fig. 1). The radius of elastic core at which plastic deformation begins can be predicted according to the Eq. 1 (Dowling, 2013):

$$r_y = \frac{\tau_o L}{G\theta} \quad (1)$$

Where:

$r_y$  = Yield radius

$\tau_o$  = The shear yield strength

$L$  = Length of cylindrical specimen

$\theta$  = The angle of twist, measured in radians at yield occurs

$G$  = Modulus of rigidity

The applied torque in torsion test can be divided into two stages, elastic torque that acting over elastic core and plastic torque that acting over plastic region outside of core and calculated by the following Eq. 2:

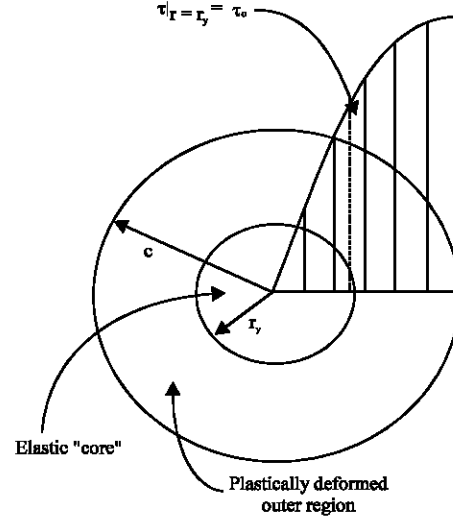


Fig. 1: Shear stress distribution in the shaft of circular cross-section through

$$T_{total} = T_{elastic} + T_{plastic} \quad (2)$$

The elastic torque is determined by elastic core where  $0 < r < r_y$ , therefore:

$$T_{elastic} = \frac{\pi \tau_o r_y^3}{2} \quad (3)$$

When the plastic region is determined as  $r_y < r < c$ , the plastic torque can becalculated using following Eq. 4:

$$T_{plastic} = \frac{2\pi h}{\sqrt{3}(n+3)} \left( \frac{\theta}{\sqrt{3}L} \right)^n \left[ c^{n+3} - r_y^{n+3} \right] \quad (4)$$

Where:

$H$  = Strength coefficient

$n$  = Strain hardening exponent) material properties measured during the tension test

$c$  = Outer radius

## MATERIALS AND METHODS

### Experimental procedure

**Material:** Material was used in this study is AA7178-T6. Chemical composition analysis of this alloy is shown in Table 1.

**Tensile test:** Mechanical properties of alloy were determined by tensile test. Figure 2 shows the relationship between stress-strain of alloy. Table 2 shows the values of  $H$  and  $n$  obtained through true stress-true strain curve in addition other some mechanical properties.

Table 1: Chemical composition of AA7178-T6

| Element (%) | Al        | Zn      | Mg      | Cu      | Si       | Fe       | Cd        | P         | Ca        |
|-------------|-----------|---------|---------|---------|----------|----------|-----------|-----------|-----------|
| Standard    | 85.3-89.5 | 6.3-7.3 | 2.4-3.1 | 1.6-2.4 | Max. 0.4 | Max. 0.5 | Max. 0.15 | Max. 0.05 | Max. 0.05 |
| Actual      | 85.94     | 8.461   | 2.484   | 2.336   | 0.273    | 0.244    | 0.196     | 0.033     | 0.028     |

Table 2: Mechanical properties of AA7178-T6

| Property | Ultimate tensile strength ( $\sigma_u$ ) (MPa) | Yield stress ( $\sigma_y$ ) (MPa) | Elongation (%) | Coefficient of strength (H) (MPa) | Exponent of strain hardening (n) | Modulus of rigidity (G)GPa | Poisson's Ratio (v) |
|----------|--|-----------------------------------|----------------|-----------------------------------|----------------------------------|----------------------------|---------------------|
| Nominal  | 607  | 538                               | 11             | -                                 | -                                | 71.7                       | 0.33                |
| Measured | 604.55   | 487.13                            | 14             | 820.71                            | 0.13                             | -                          | -                   |

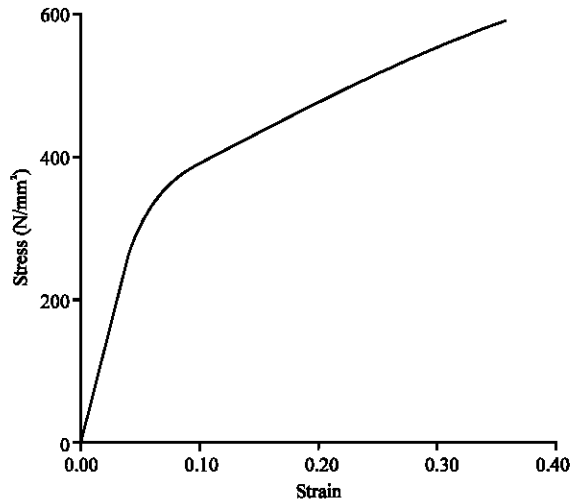


Fig. 2: Stress-strain relationship obtained from a torsion test by tensile test (Dowling, 2013)

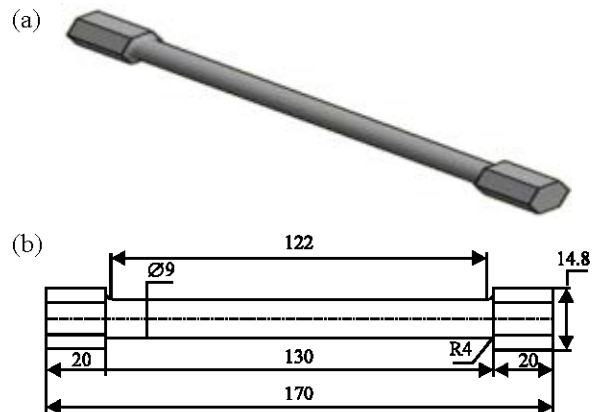


Fig. 3: Geometric and dimensions of torsion test specimen (dimension in mm)

**Torsion test:** Specimens of torsion test were manufactured according to standard specification for testing (ASTM standard D790-02). Figure 3 shows the geometric and dimensions of these specimens.

**Shot-peening:** Torsion specimens were shot-peened for different times: 2.5, 5, 10, 15, 20, 25, 30 min as three

specimens for each time with steel balls having a diameter of 1.25 mm at constant velocity and the amount of balls is 1 kg weighted.

**Residual stresses measurement:** To measure residual stresses on the surface of torsion specimens according to shot-peening time, XRD-6000 device was used for this purpose. The data of this test represents the average value of three specimens at each shot-peening time.

**Surface roughness measurement:** To evaluate the influence of specimen surface with shot-peening time, surface roughness measurement was carried out using Mahr Federal device.

## RESULTS AND DISCUSSION

**Effect of residual stresses and surface roughness:** Residual stresses and surface roughness give indication about the shot-peening effectiveness on specimen surface. Shot-peening usually leaves compression residual stress on the surface of specimen and causes an increase in surface roughness. The shot-peening process brings about the strengthening of the surface layer, resulting in a rough surface with a high ability to resist plastic deformation. Table 3 contains values of those parameters according to the time of shot-peening. It is observed that the surface roughness increases whenever shot-peening time increases because of increasing shot intensity and shot coverage while compression residual stresses begin with a high value at 2.5 min of shot-peening and decrease to reach a minimum value at 30 min. This is because over-peening can cause cracks even on the surface and inversion of stress thus reducing the compressive stress (Bhuvraghan *et al.*, 2010). Plasticity effect becomes significant when compressive residual stresses exist (Bae *et al.*, 2014). Generally, shot-peening causes plastic deformation which leads to an increase in surface hardness and strength of material, resulting in resistance to plastic deformation in torsion test.

**Effect of shot peening time on shear stress and shear strain:** The effect of shot-peening time on shear stress

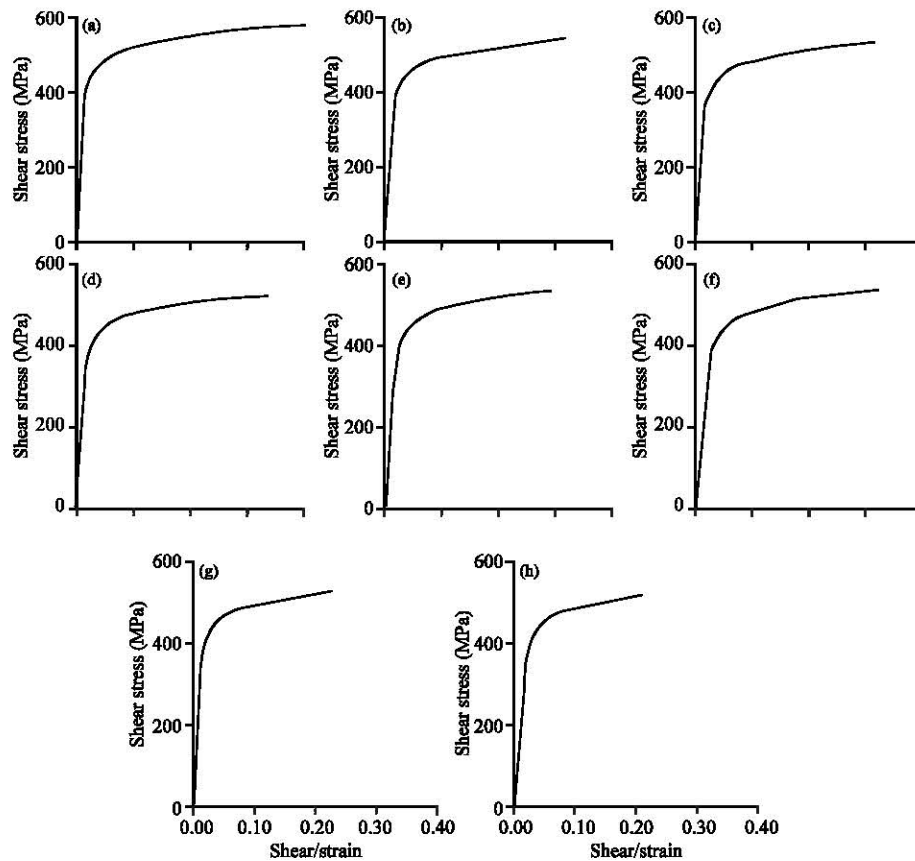


Fig. 4: Shear stress-shear strain relationship of alloy at different shot peening time: a) Without shot-peening; b) Shot-peening at 2.5 min; c) Shot-peening at 5 min; d) Shot-peening at 10 min; e) Shot-peening at 15 min; f) Shot-peening at 20 min; g) Shot-peening at 25 min and h) Shot-peening at 30 min

Table 3: Residual stress and surface roughness

| Time of shot-peening (min) | Residual stress (MPa) | Surface roughness $R_a$ ( $\mu\text{m}$ ) |
|----------------------------|-----------------------|---|
| Without peening            | -6.855                |   |
| 2.5                        | -45.288               | 2.06                                      |
| 5                          | -44.120               | 2.34                                      |
| 10                         | -43.468               | 2.58                                      |
| 15                         | -41.544               | 2.66                                      |
| 20                         | -26.368               | 2.84                                      |
| 25                         | -18.997               | 3.06                                      |
| 30                         | -17.808               | 3.10                                      |

Table 4: Parameters of torsion test

| Shot time (min) | $\theta_f$ (rad) | $\theta_o$ (rad) | $\tau_o$ (MPa) | $r_y$ (mm) | $T_{elastic}$ (Nm) | $T_{plastic}$ (Nm) |
|-----------------|------------------|------------------|----------------|------------|--------------------|--------------------|
| Without shot    | 10.728           | 0.568            | 384.44         | 3.020      | 16.624             | 50.753             |
| 2.5             | 9.949            | 0.527            | 384.44         | 3.250      | 20.719             | 45.007             |
| 5               | 8.526            | 0.541            | 384.44         | 3.170      | 19.226             | 45.963             |
| 10              | 8.765            | 0.473            | 349.49         | 3.290      | 19.540             | 43.280             |
| 15              | 7.566            | 0.541            | 377.45         | 3.110      | 17.825             | 46.555             |
| 20              | 8.198            | 0.541            | 390.31         | 3.220      | 20.458             | 42.213             |
| 25              | 6.214            | 0.586            | 384.44         | 2.927      | 15.135             | 48.948             |
| 30              | 5.887            | 0.554            | 377.45         | 3.040      | 16.650             | 46.446             |

and shear strain of AA7178-T6 alloy is illustrated in Fig. 4. It is obvious that the shear strain clearly decreased when the time of shot-peening increase while the shear stress values closed to each other. The explanation of this result belongs to the plastic deformation of the specimen surface caused by shot-peening which lead to increase the strength of alloy and resist plastic deformation then fail at less angle of twist whenever shot-peening time increased. The reduction of shear strain value at 30 min time reached 45% while shear stress decreased by 3.84% in comparison with the specimen without peening. Table 4 contains the values of angle of twist at yield ( $\theta_o$ ),

angle of twist at failure ( $\theta_f$ ), shear stress at yield ( $\tau_o$ ), radius of elastic core ( $r_y$ ), elastic torque and plastic torque. These values pointed to the shot-peening time effectiveness in decrease the angle of twist at failure and plastic torque while small variation appeared in the other parameters ( $\theta_o$ ,  $r_y$ ,  $\tau_o$  and  $T_{elastic}$ ) in comparison with their values of specimen without shot-peening. This means that the shot-peening has small effect in elastic stage of torsion test while plastic stage appeared more affect by this process. The increasing of shot-peening time, especially, at 30 min. decreased plastic torque compared to the specimen without shot-peening because high

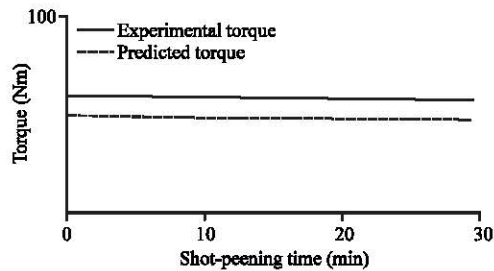


Fig. 5: Experimental and predicted torque

peening intensity occur when shot-peening time increase and create deformation surface layer which increased the strength of alloy and resist plastic deformation in torsion test. The plastic torque at 30 min. shot-peening time decreased by about 10% compared with plastic torque of specimen without shot-peening. The difference between predicted torque and experimental torque values is 14% in average as shown in Fig. 5. The figure appeared small reduction of torque when shot-peening time increased and the average is 3.84 and 6.35% experimentally and theoretically, respectively.

## CONCLUSION

Increasing of shot-peening time carried out on AA7178-T6 alloy lead to increase of plastic deformation resistance in torsion test. Shot-peening process carried out on AA7178-T6 alloy effected in plastic stage more than elastic stage of torsion test of alloy. Shear strain was decreased whenever shot-peening time increased while small variation occur in shear stress through torsion test of alloy. Max. reduction of shear strain and shear stress are 45 and 3.84%, respectively. Plastic torque predicted for specimen peened at 30 min. time was decreased by 10% compared with its value of specimen without peening while elastic torque predicted remain in the same value. Predicted torque for shot specimens less than experimental torque by 14% in average of this alloy. Experimental and theoretical torque decrease whenever shot-peening time increase by 3.84 and 6.35%, respectively.

## ACKNOWLEDGEMENT

The researchers would like to thank anyone who helped or supported in accomplishment of this research.

## REFERENCES

Albuquerque, M.D.C.F.D. and J.D.A. Rodrigues, 2008. Study of the dimensions of double-torsion test specimens. *Mater. Res.*, 11: 281-288.

Bae, H., H. Diep and M. Ramulu, 2014. Influence of shot peening coverage on residual stresses induced in aluminum alloy 7050-T7 45. *Proceedings of the 12th International Conference on Shot Peening ICSP*, September 15-18, 2014, ICSP, Goslar, Germany, pp: 282-287.

Barthelat, F., K. Malukhin and H. Espinosa, 2002. Quasi-Static and Dynamic Torsion Testing of Ceramic Micro and Nano-structured Coatings using Speckle Photography. In: *Recent Advances in Experimental Mechanics*, Gdoutos, E.E. (Ed.). Springer, Dordrecht, Netherlands, ISBN: 978-1-4020-0683-8, pp: 75-84.

Bhuvaraghan, B., S.M. Srinivasan and B. Maffeo, 2010. Optimization of the fatigue strength of materials due to shot peening: A survey. *Intl. J. Struct. Changes Solids*, 2: 33-63.

Bidulska, J., T. Kvackaj, R. Bidulsky, M. Cabbibo and E. Evangelista, 2007. Effect of low strain rate on formability of Aluminium alloy. *Metalurgija*, 46: 157-159.

Bressan, J.D., 2007. Plastic behavior and fracture of Aluminum and copper in torsion tests. *AIP. Conf. Proc.*, 907: 521-526.

Diani, J., C. Fredy, P. Gilormini, Y. Merckel and G. Regnier *et al.*, 2011. A torsion test for the study of the large deformation recovery of shape memory polymers. *Polym. Test.*, 30: 335-341.

Dowling, N.E., 2013. *Mechanical Behavior of Materials: Engineering Methods for Deformation, Fracture and Fatigue*. 4th Edn., Pearson, London, UK., ISBN:9780131395060, Pages: 936.

Jonathan, A.S., R. Mitedin, E. Lara-Curzio and N.J. George, 2008. Fracture Toughness of Thin Plates by the Double-Torsion Test Method. In: *Mechanical Properties and Performance of Engineering Ceramics II: Ceramic Engineering and Science Proceedings*, Jonathan, A.S., R. Mitedin, E. Lara-Curzio and N.J. George (Eds.). John Wiley & Sons, Hoboken, New Jersey, USA., pp: 63-73.

Meng, Q. and G.S. Frankel, 2004. Effect of Cu content on corrosion behavior of 7xxx series aluminum alloys. *J. Electrochem. Soc.*, 151: B271-B283.

Mossakovsky, P.A., F.K. Antonov and L.A. Kostyreva, 2011. Investigation of failure criterion in dynamic torsion tests with solid cylindrical specimens. *Proceedings of the 8th European International Conference on LS-DYNA Users*, May 23-34, 2011, OECD, Strasbourg, France, pp: 1-6.

- Nayak, S.Y., N.M. Amin, S.S. Heckadka, V. Shenoya and C S. Prakash *et al.*, 2018. Design, fabrication and testing of carbon fiber reinforced epoxy drive shaft for all terrain vehicle using filament winding. Proceedings of the International Conferences on MATEC Web Vol. 153, February 26, 2018, EDP Sciences, Les Ulis, France, pp: 1-5.
- Orduna, A. and P.B. Lourenco, 2005. Three-dimensional limit analysis of rigid blocks assemblages; Part I: Torsion failure on frictional interfaces and limit analysis formulation. *Intl. J. Solids Struct.*, 42: 5140-5160.
- Patil, R.D. and P.N. Gore, 2013. Review the effect of specimen geometry on torsion test results. *Intl. J. Innovative Res. Sci. Eng. Technol.*, 2: 7567-7574.
- Roesler, C.R.M., G.V. Salmoria, A.D.O. More, J.M. Vassoler and E.A. Fancello, 2014. Torsion test method for mechanical characterization of PLDLA 70/30 ACL interference screws. *Polym. Test.*, 34: 34-41.
- Saborowski, E., M. Scholze, T. Lindner and T. Lampke, 2017. A numerical and experimental comparison of test methods for the shear strength in hybrid metal-thermoplastic-compounds. Proceedings of the IOP International Conference on Series: Materials Science and Engineering Vol. 181, March 16-17, 2017, IOP Publishing, Bristol, UK., pp: 1-13.
- Schiltges, G., D. Gsell and J. Dual, 1998. Torsional tests on microstructures: Two methods to determine shear-moduli. *Microsyst. Technol.*, 5: 22-29.
- Vainikka, O., J. Halinen, M. Pajula, A. Sarhajuoma and P. Kiviluoma *et al.*, 2015. Implementation of a torsion testing device for 3D-printed plastic tubes. Proceedings of the 10th International Conference on DAAAM Baltic Industrial Engineering, May 12-13, 2015, Tallinn University of Technology, Tallinn, Estonia, pp: 205-210.